MAX-PLANCK-INSTITUT
FÜR PLASMAPHYSIK

Electron-only reconnection and ion heating in 3D3V hybrid-Vlasov plasma turbulence

Transalpine Workshop, Nice

Camille Granier

With:
S. Cerri – *Laboratoire Lagrange*
F. Jenko – *IPP*

PLASMA
ASTRO

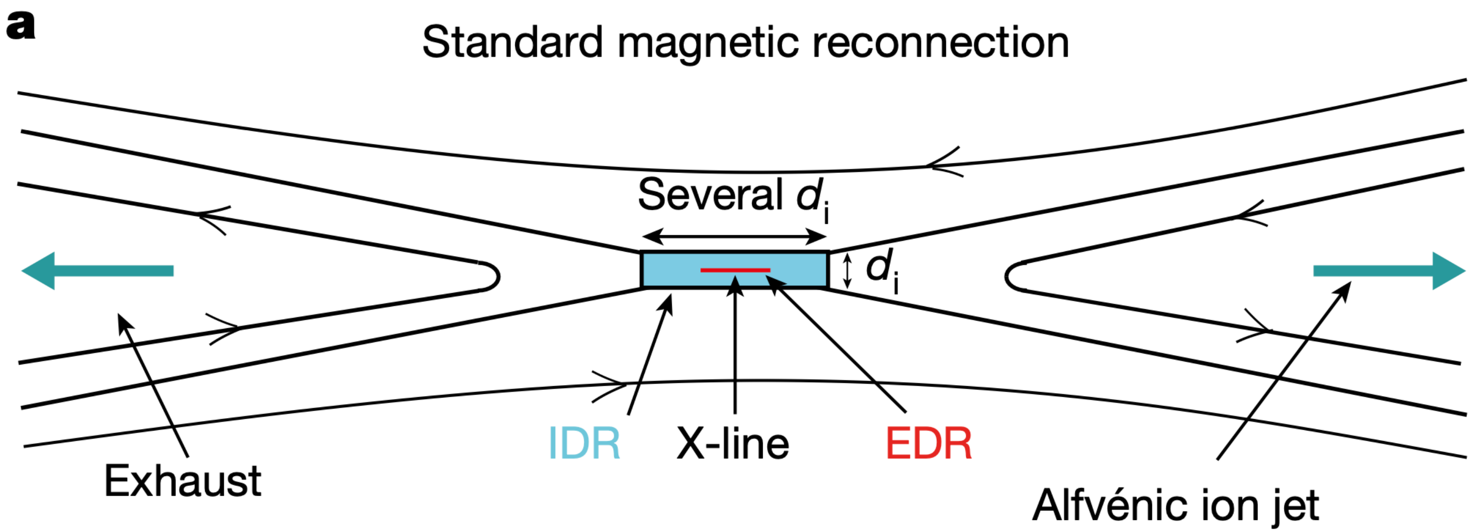
a
Standard magnetic reconnection
Several d_i
d_i
IDR
X-line
EDR
Exhaust
Alfvénic ion jet

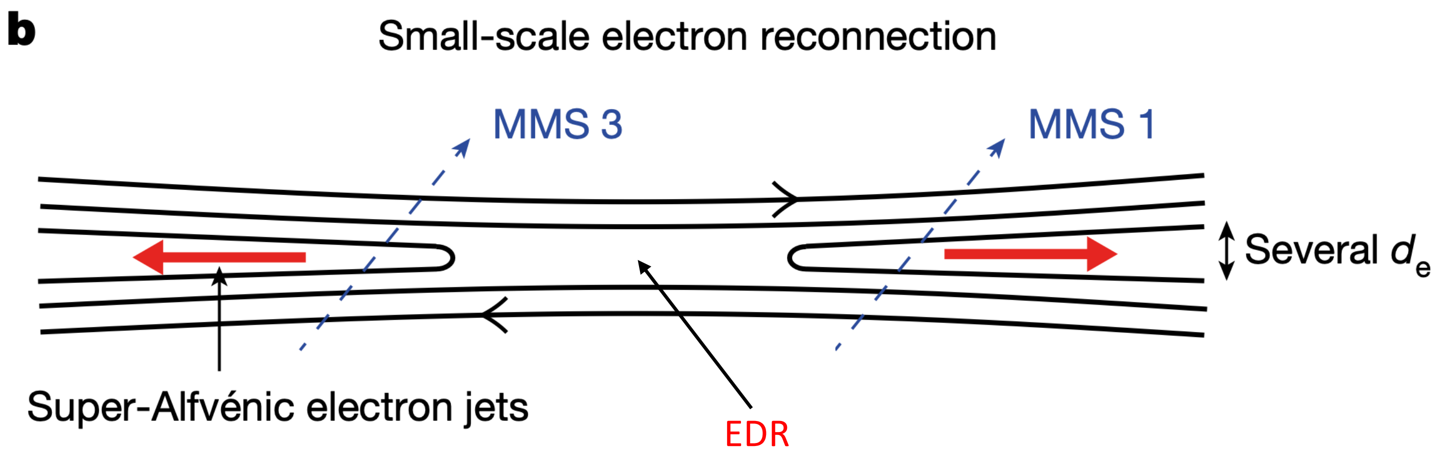
b
Small-scale electron reconnection
MMS 3
MMS 1
Several d_e
Super-Alfvénic electron jets
EDR

Magnetosheath Observations:

Phan et al. 2018. *Electron magnetic reconnection without ion coupling in Earth's turbulent magnetosheath*

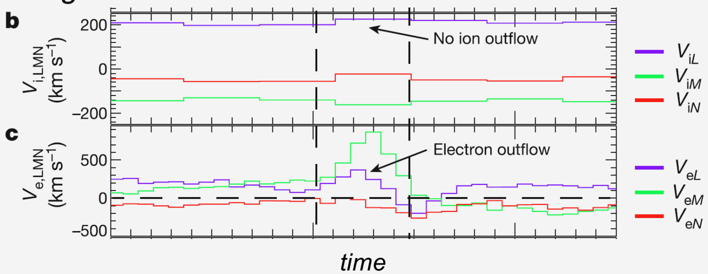

Stawarz et al. 2023

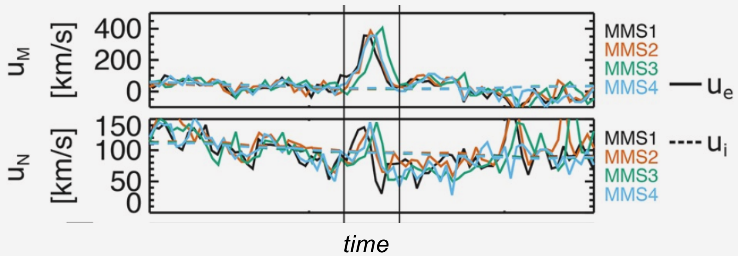

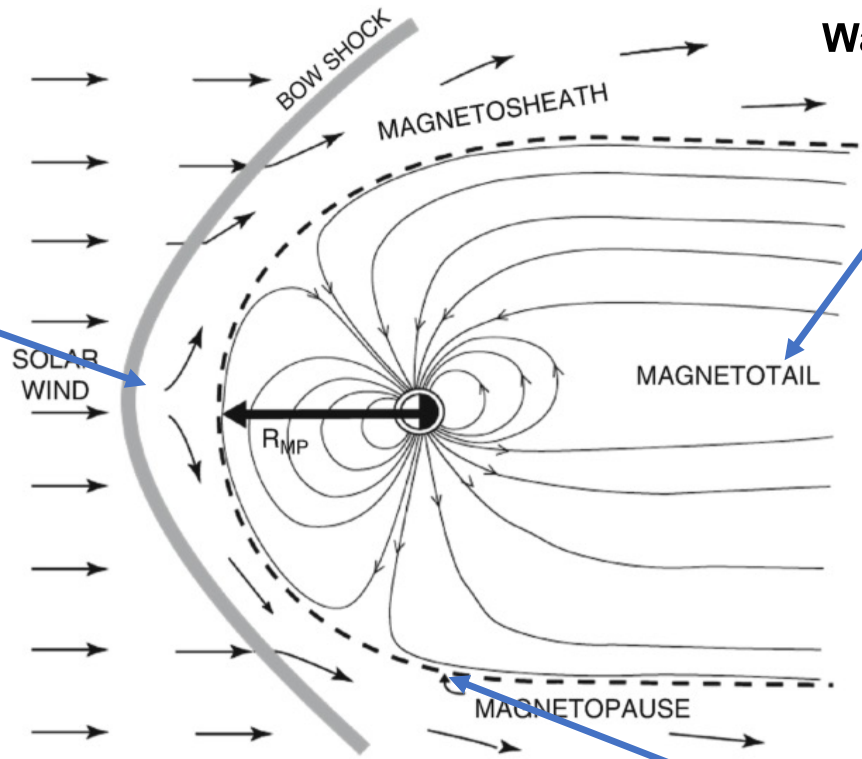

Wang et al. 2020

Huang et al. 2021

Numerical experiments:

- Sharma Pyakurel et al. (2019).
  2D Particle-in-Cell (PIC) simulations have suggested that when the current sheet's length is less than approximately $10d_i$.

- Other 2D references: Califano et al. (2020), Arro et al. (2020), Vega et al. (2020).

Sharma Pyakurel et al. (2019)

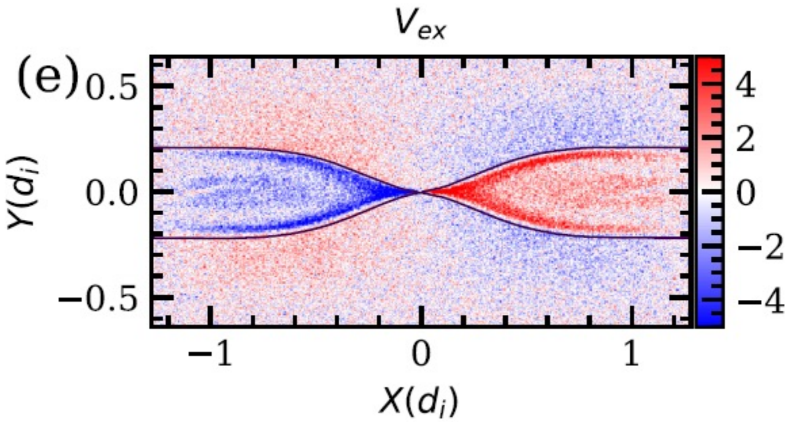

Theories:

- Mallet (2020): transition from ion coupled to electron-only reconnection for $\frac{L_{cs}}{\delta_{cs}} < 10$ and $\delta_{cs} < \rho_s$.

- Betar & Del Sarto (2023): certain aspects of such reconnection regime can be accurately described by EMHD equations.

Califano et al. (2020)

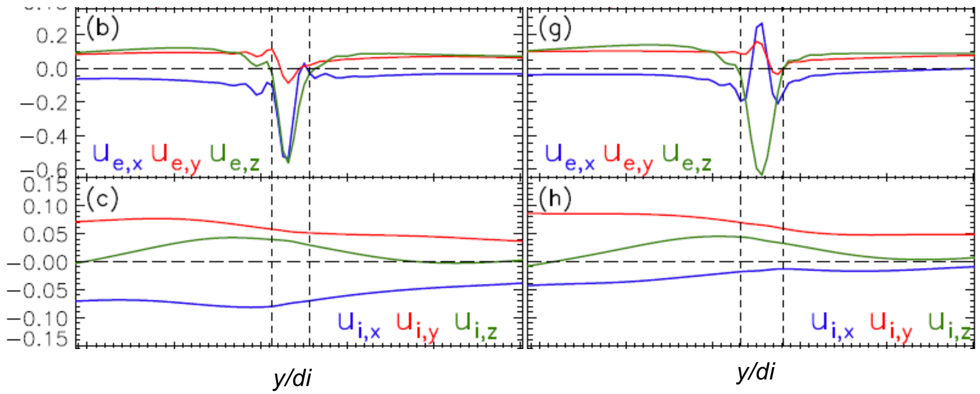

Numer

- Shar

- Othe
(202

Theori

- Malle
only

- Beta
reco
EMH

Conclusion for 2D:

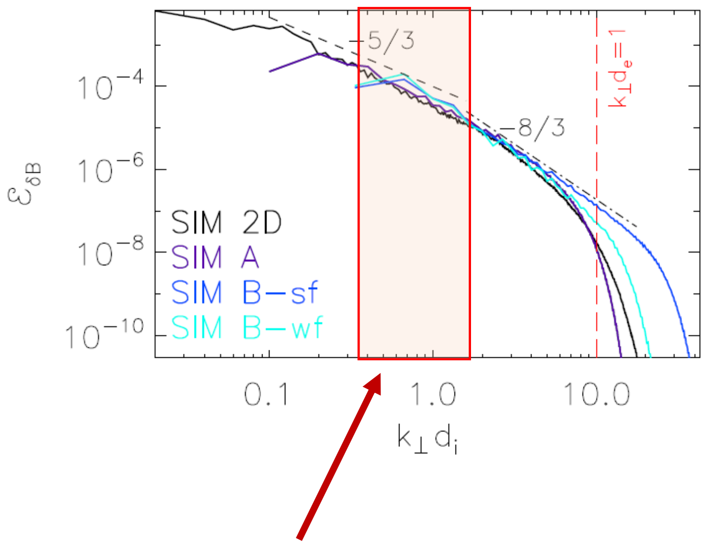

Injection scale has to be d_i

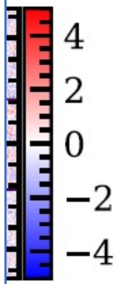

y/di

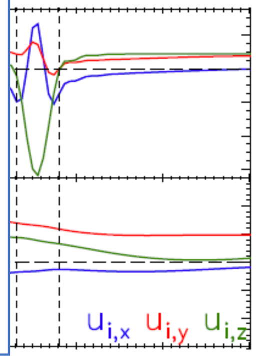

Eulerian Hybrid Vlasov Maxwell

Pros:

- Ion microscale phenomena + some for the e^-.
- «Adaptable» electron closure.
- Less noisy than PIC.

Cons:

- Typically more expensive than PIC.
- Lack of electron Landau damping.
- Less analytically tractable -> increased compexity compared to fluid/gyrofluid.

Quasi-neutral, kinetic ions, fluid electrons (Valentini 2007).

$$\frac{\partial f_\mathrm{i}}{\partial t} + \boldsymbol{v} \cdot \nabla f_\mathrm{i} + (\boldsymbol{E} + \boldsymbol{v} \times \boldsymbol{B}) \cdot \frac{\partial f_\mathrm{i}}{\partial \boldsymbol{v}} = 0,$$

$$\left(1 - d_\mathrm{e}^2 \nabla^2\right) \boldsymbol{E} = -\boldsymbol{u}_\mathrm{i} \times \boldsymbol{B} + \frac{\boldsymbol{J} \times \boldsymbol{B}}{n} - \frac{\nabla P_\mathrm{e}}{n} + \frac{d_\mathrm{e}^2}{n} \nabla \cdot \left(\boldsymbol{u}_\mathrm{i} \boldsymbol{J} + \boldsymbol{J} \boldsymbol{u}_\mathrm{i} - \frac{\boldsymbol{J}\boldsymbol{J}}{n}\right)$$

Isothermal electrons $P_e = n\, T_{0e}$

MAX PLANCK
COMPUTING & DATA FACILITY

Eulerian Hybrid Vlasov Maxwell

Pros:

- Ion microscale phenomena + some for the e^-.
- «Adaptable» electron closure.
- Less noisy than PIC.

Cons:

- Typically more expensive than PIC.
- Lack of electron Landau damping.
- Less analytically tractable -> increased compexity compared to fluid/gyrofluid.

Quasi-neutral, kinetic ions, fluid electrons (Valentini 2007).

$$\frac{\partial f_\mathrm{i}}{\partial t} + \boldsymbol{v} \cdot \nabla f_\mathrm{i} + (\boldsymbol{E} + \boldsymbol{v} \times \boldsymbol{B}) \cdot \frac{\partial f_\mathrm{i}}{\partial \boldsymbol{v}} = 0,$$

$$\left(1 - d_\mathrm{e}^2 \nabla^2\right) \boldsymbol{E} = -\boldsymbol{u}_\mathrm{i} \times \boldsymbol{B} + \frac{\boldsymbol{J} \times \boldsymbol{B}}{n} - \frac{\nabla P_\mathrm{e}}{n} + \frac{d_\mathrm{e}^2}{n} \nabla \cdot \left(\boldsymbol{u}_\mathrm{i} \boldsymbol{J} + \boldsymbol{J} \boldsymbol{u}_\mathrm{i} - \frac{\boldsymbol{J}\boldsymbol{J}}{n} \right)$$

Isothermal electrons $P_e = n\, T_{0e}$

Assumptions quasi-neutrality and no displacement current:

$$\partial \boldsymbol{J} / \partial t \approx c^2 \nabla^2 \boldsymbol{E} / 4\pi$$

Mass ratio: $\frac{m_i}{m_e} = 100$

Ion beta: $\beta_i = 0.25, \; 1, \; 4$

Electron beta: $\beta_e = 0.1 \quad \rightarrow \quad (\rho_e \ll d_e)$

Injection:

- At scales: $0.33 < k_{inj} d_i < 1$.
- $\delta B / B_0 = 0.5$, and converges to $\delta B / B_0 = 0.3$

Reproducing Earth's bow shock conditions.

Resolution in Real Space:

- Grid Resolution: 256^3 grid Points
- Box Size: $L_\perp = L_\parallel = 3\times 2\,\pi\, \mathrm{d_i}$

Resolution in Velocity Space:

- Grid of 51^3 or 57^3 uniformly distributed points
- Velocity Domain Limit $\quad v_{max} = \pm 5 - 7 \, v_{thi}$

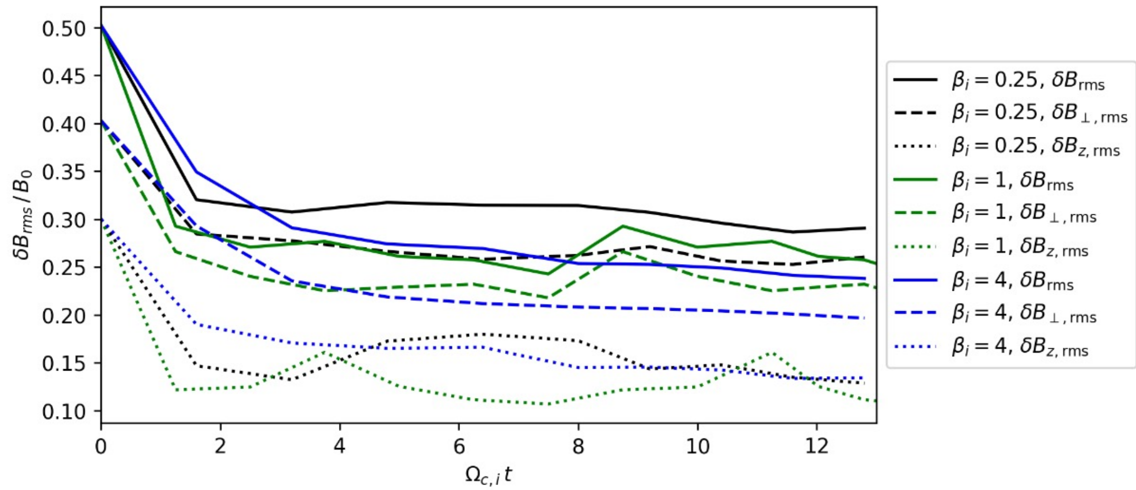

Spectral properties.

Turbulence fully develloped when J^{rms} reaches a maximum.

Small structures are visible at the ion inertia scale.

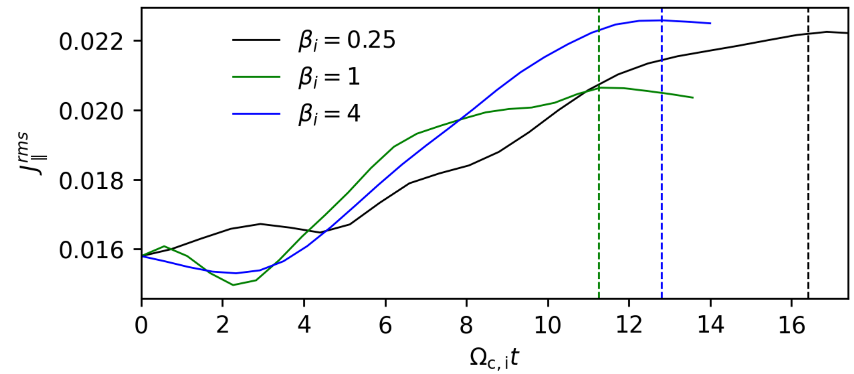

$|\boldsymbol{B}_\perp|$

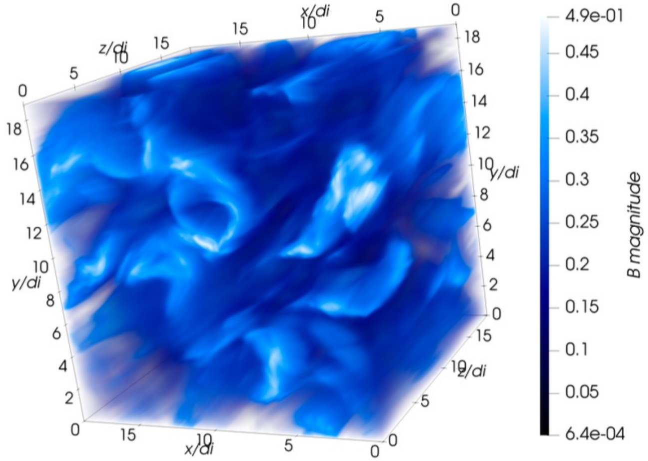

$|\boldsymbol{E}'| = |\boldsymbol{E} + \boldsymbol{u}_e \times \boldsymbol{B}|$

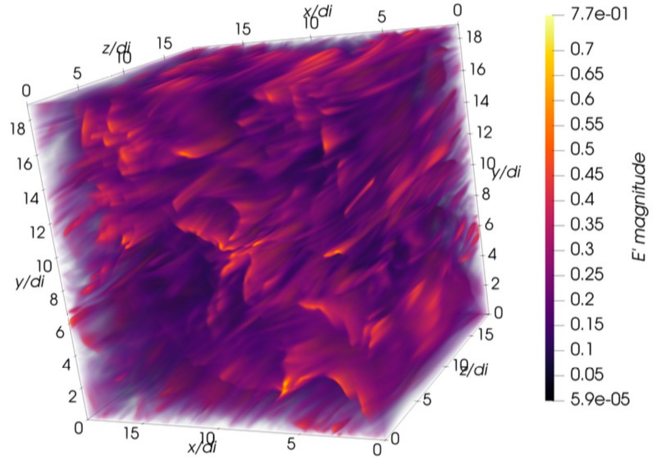

$|\boldsymbol{J}|$

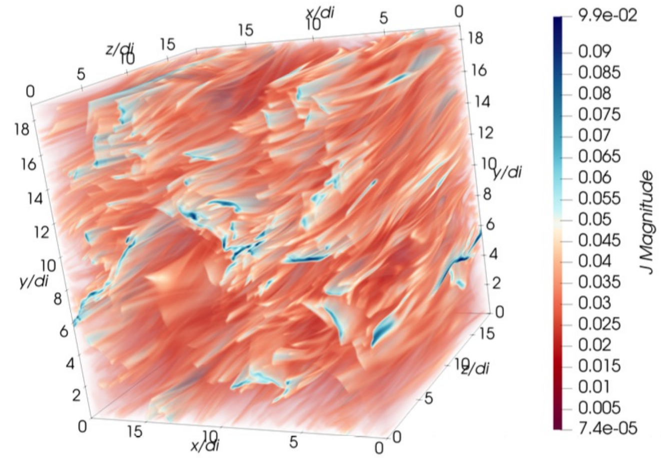

Spectral properties.

Magnetic compressibility at sub-ion scale and for hot ions *(Chen & Boldyrev (2017))*:

- Transition from KAW to IKAW: $\frac{\delta B_{\parallel}^2}{\delta B_{\perp}^2} = \frac{1 + k_{\perp}^2 d_{\mathrm{e}}^2}{1 + \frac{2}{\beta_{\mathrm{i}}} + k_{\perp}^2 d_{\mathrm{e}}^2}$
- For inertial Whistler Waves, and for $k_{\parallel}^2\, d_i^2 \gg k_{\perp}^2 d_e^2 \sim 1$, $\frac{\delta B_{\parallel}^2}{\delta B_{\perp}^2} = \frac{1 + k_{\parallel}^2 d_{\mathrm{i}}^2 + k_{\perp}^2 d_{\mathrm{e}}^2}{k_{\parallel}^2 d_{\mathrm{i}}^2} \approx 1$

For IWW (EMHD regime), density fluctuations are negligeable, $\frac{\delta n}{n_0} \ll 1$

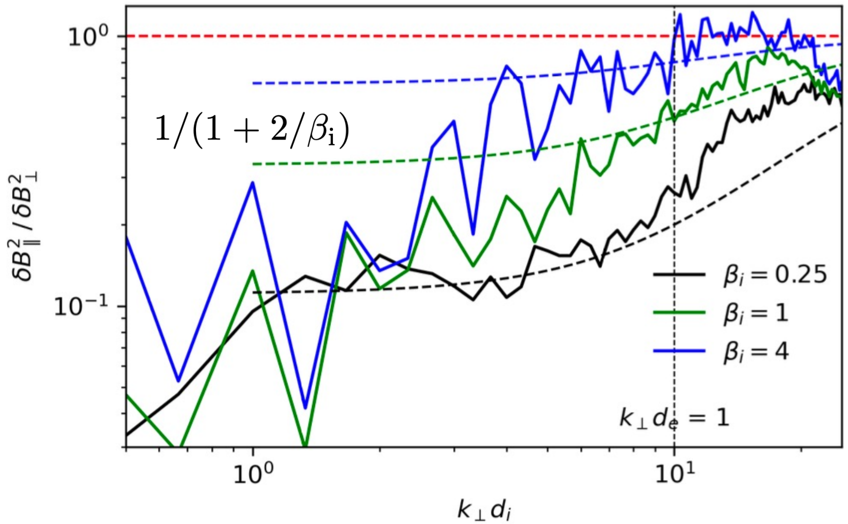

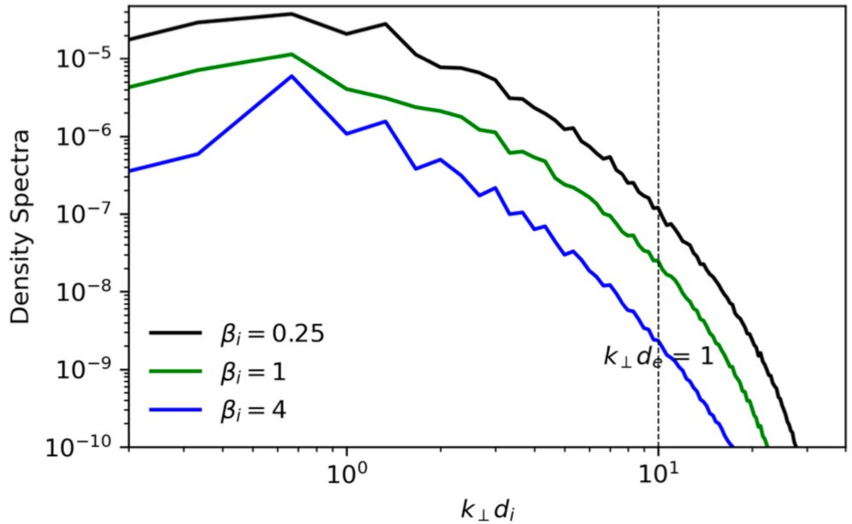

Spectral properties.

$\beta_i = 0.25$

Similar

$\beta_i = 1$

EM spectra

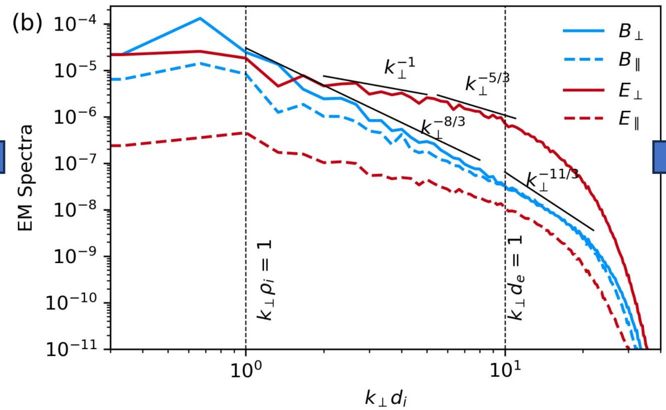

- Sub-ion scale:

$$B_\perp \propto k_\perp^{-\frac{8}{3}}, \quad E_\perp \propto k_\perp^{-1}$$

- Close to electron scale:

$$B_\perp \propto k_\perp^{-\frac{11}{3}}, \quad E_\perp \propto k_\perp^{-5/3}$$

$\beta_i = 4$

Similar

Spectral properties.

$\beta_i = 0.25$

Similar

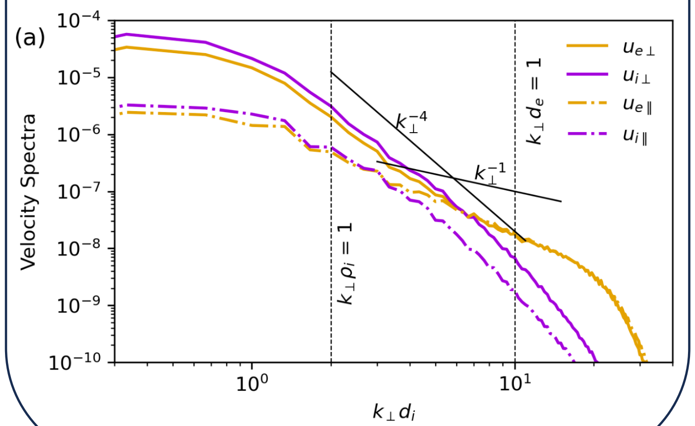

$\beta_i = 1$

EM spectra

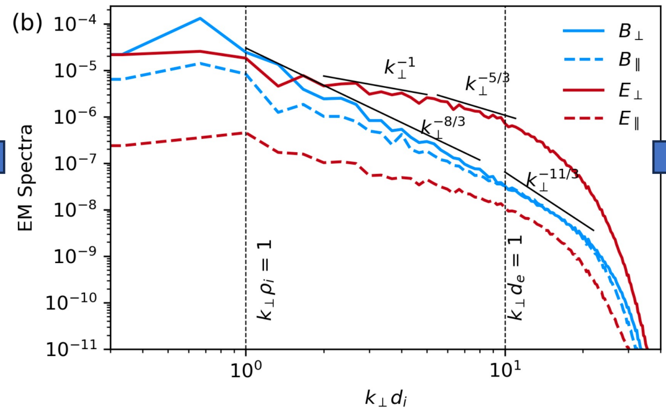

Velocity spectra

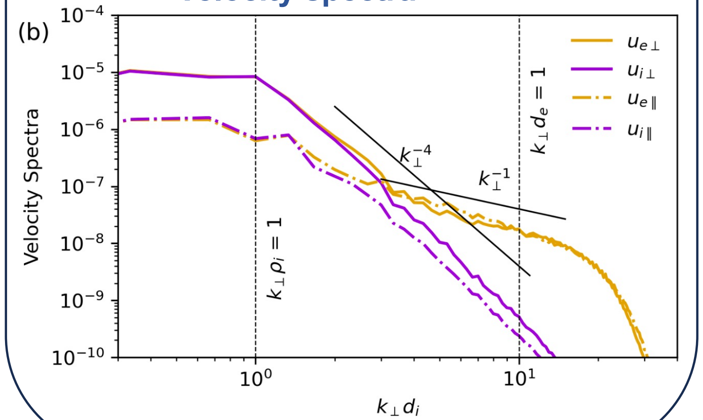

$\beta_i = 4$

Similar

Efficient decoupling!!

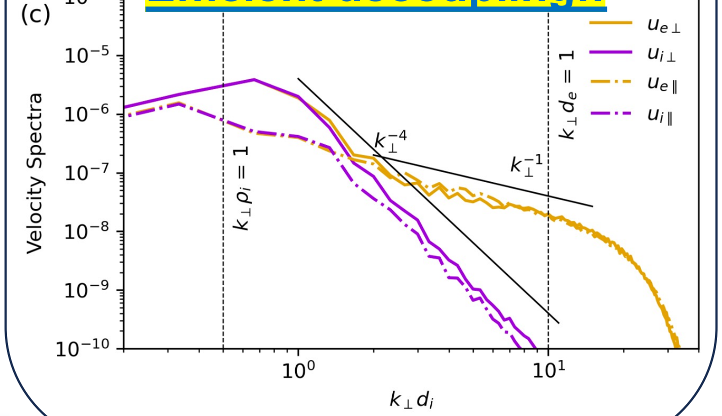

Electron-only reconnection.

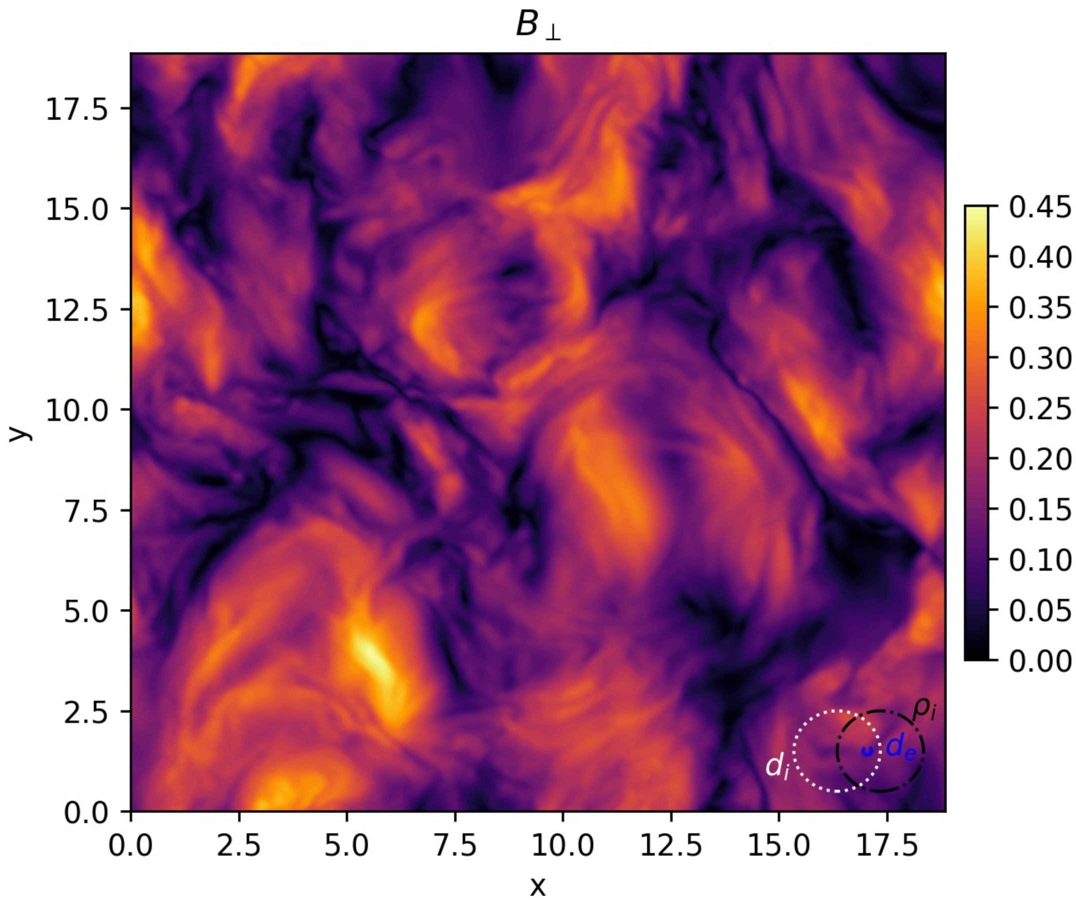

Electron-only reconnection.

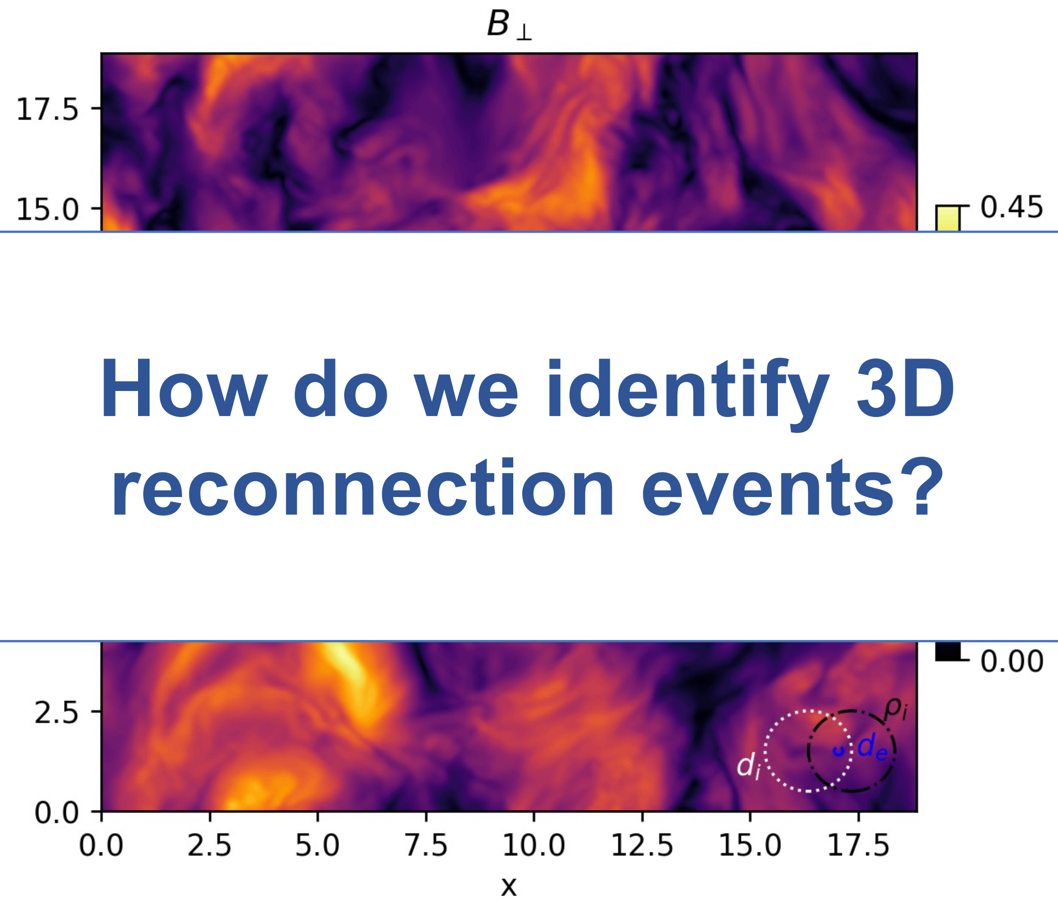

How do we identify 3D reconnection events?

Electron-only reconnection.

Signature of reconnection:

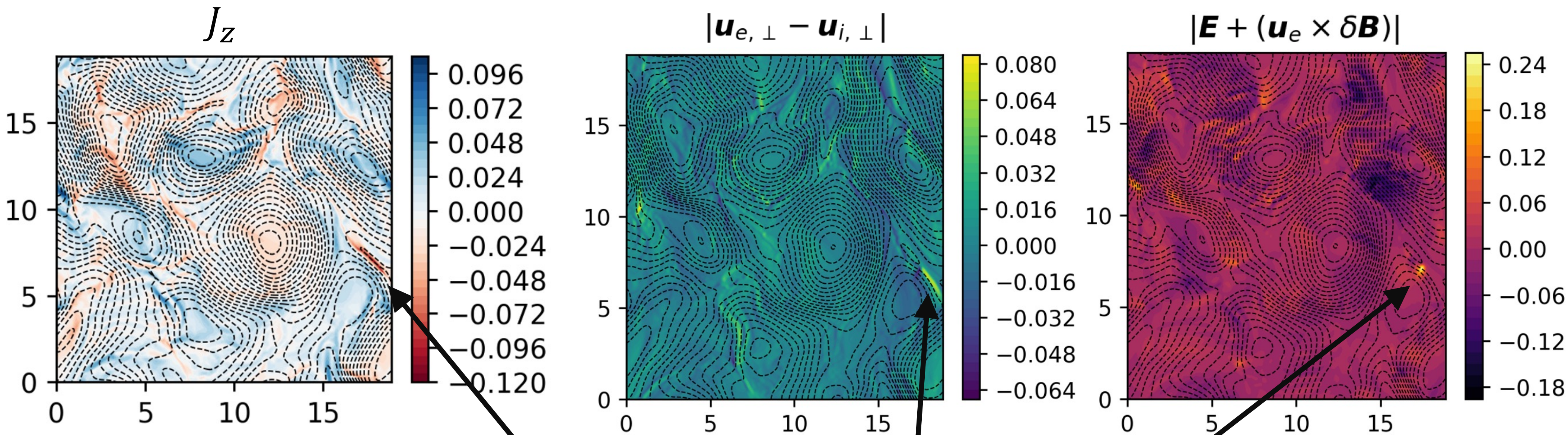

- Current sheet formation.
- Reversal of magnetic field direction.
- Plasma flow: **eventually a difference between $u_{e\perp}$ and $u_{i\perp}$.**
- Locally high electric field: related to the reconnection rate.

Electron-only reconnection.

- Electron outflows are clearly visible. Ions freely stream through without being affected.
- Outflow predominantly oriented in the perpendicular plane.
- For $\beta_i = 0.25, \rightarrow \quad l_{outf} \approx \quad 0.7\ d_i$.
- For $\beta_i = 4, \rightarrow \quad l_{outf} \approx \quad 1.5\ d_i$.

$\beta_i = 4$

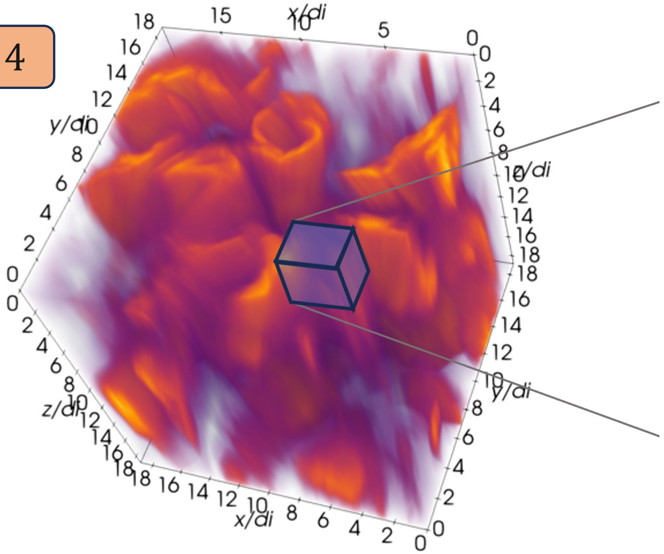

Electron velocity field:

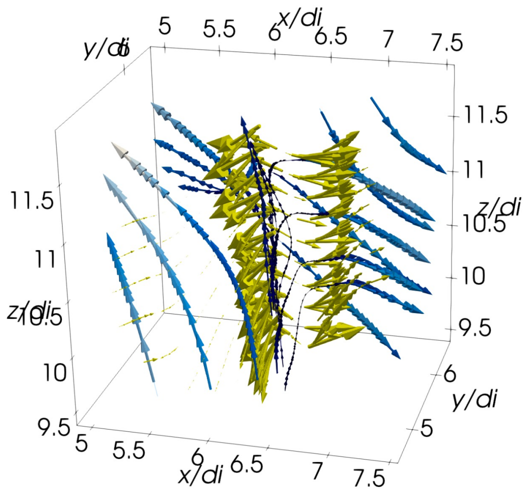

Ion velocity field:

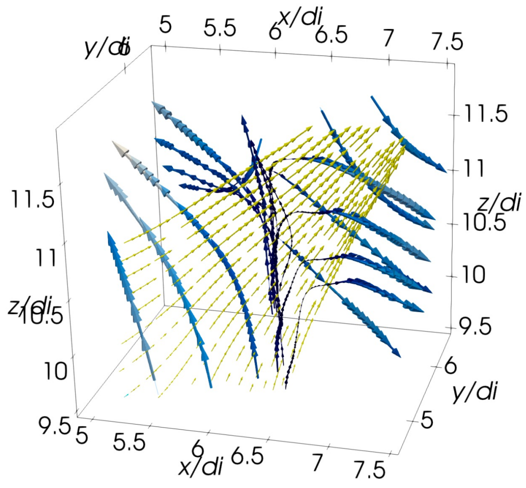

Electron-only reconnection.

$\beta_i = 0.25$

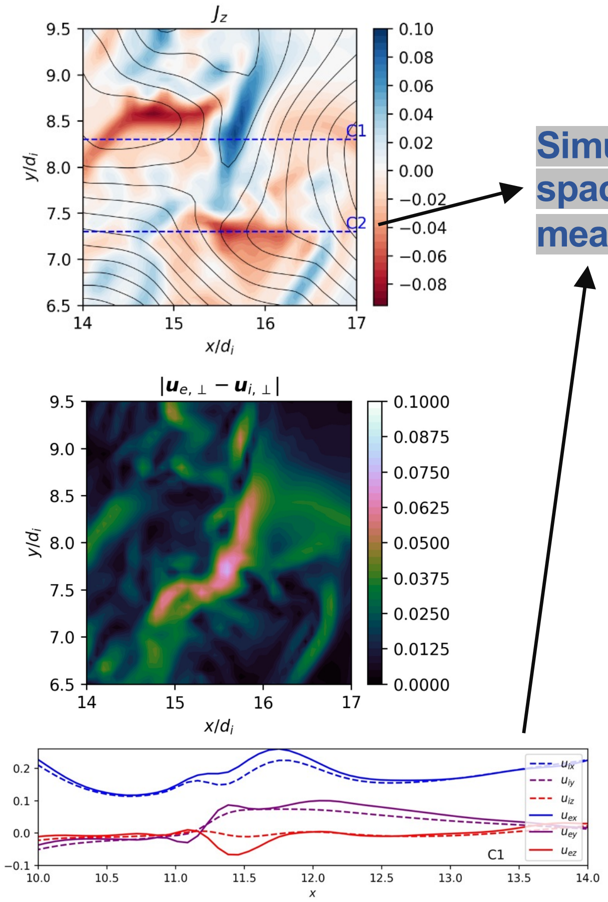

Simulating a spacecraft measurement.

$\beta_i = 1$

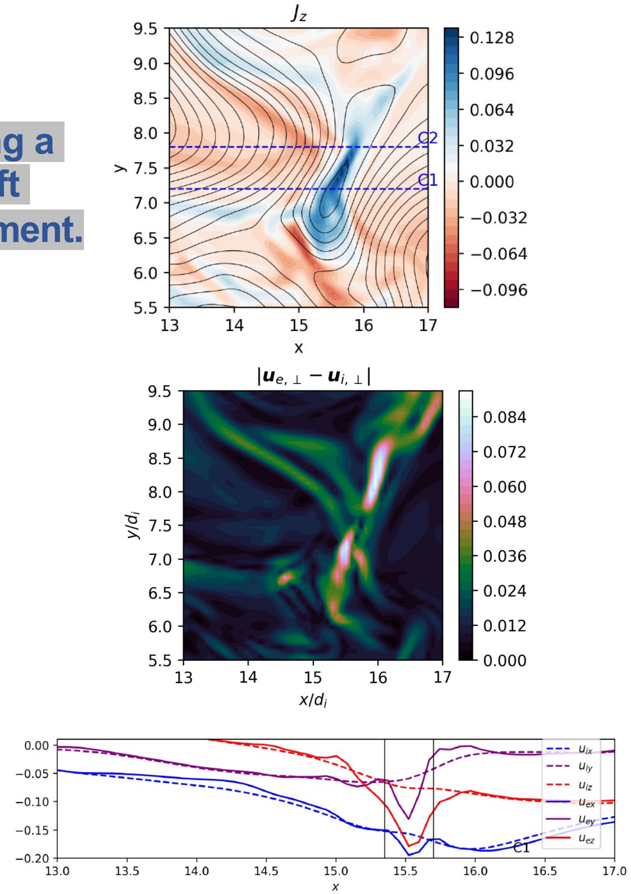

$\beta_i = 4$

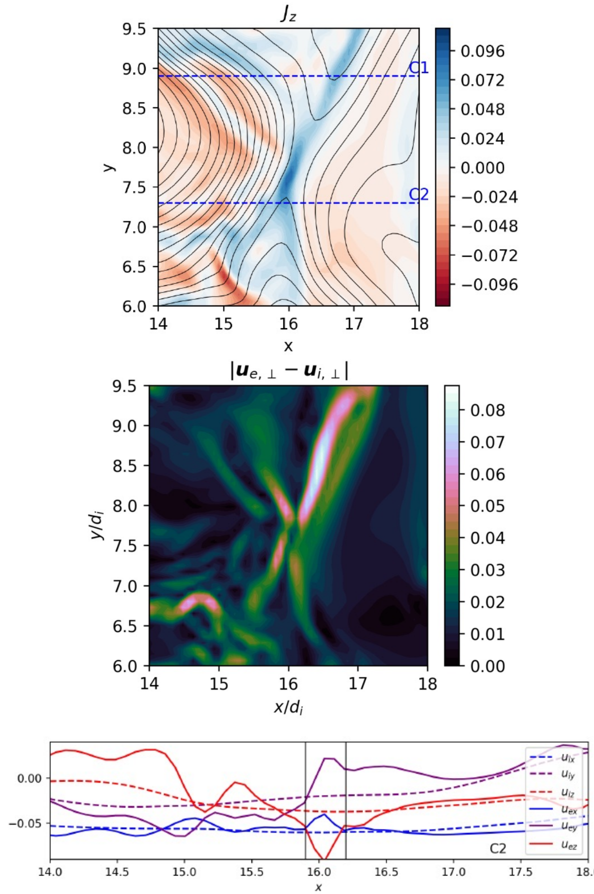

- Anisotropic heating: $T_{i,\perp} > T_{i,\parallel}$, more pronounced for small β_i.

- The distribution of $T_{i,\perp}/T_{i,\parallel}$ values show more important spread as β_i decreases. Remains in a marginally stable region bounded by the ion Cyclotron Instability (iCI) threshold.

$$T_{i,\parallel} = (\mathbf{\Pi}_i : \boldsymbol{bb})/n$$

$$T_{i,\perp} = (\mathbf{\Pi}_i : \boldsymbol{\sigma})/n$$

With $\sigma_{ij} = (\delta_{ij} - b_i b_j)/2$ the projector onto the plan perpendicular to $\boldsymbol{B}$.

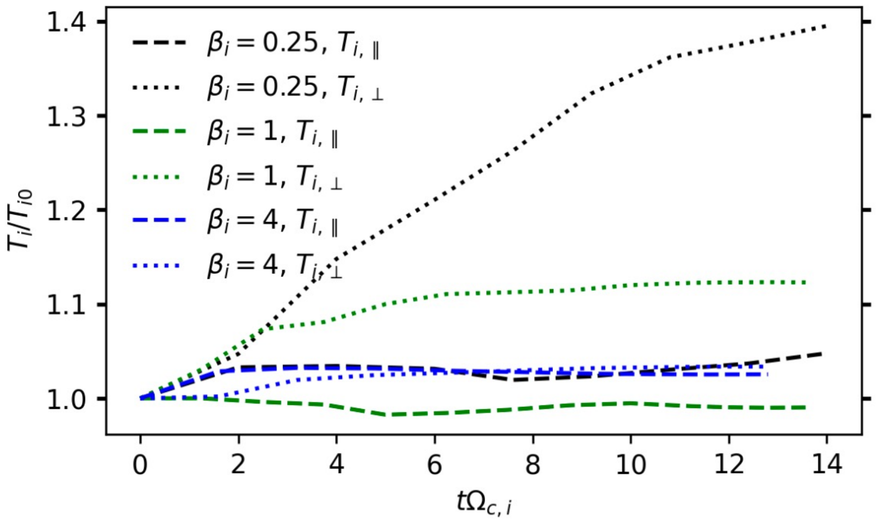

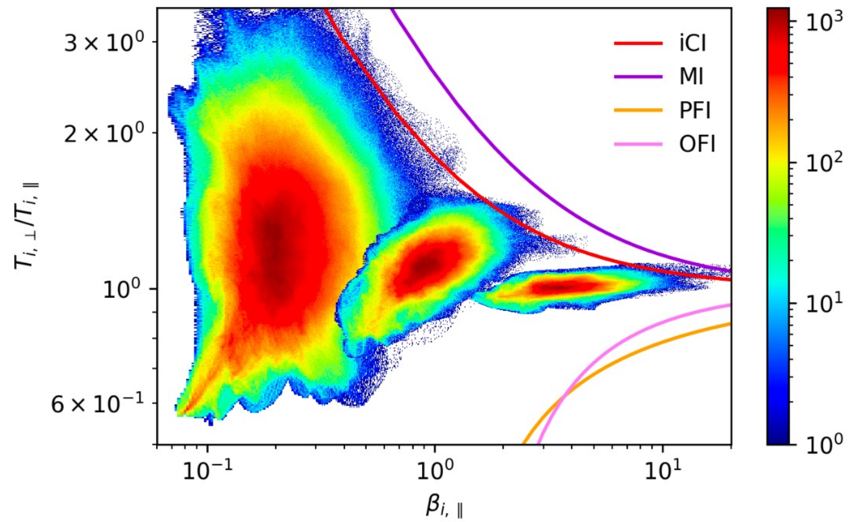

- A larger fraction of the cascading magnetic energy is converted into ion heating as β_i increases.

- Ratio $\Delta E_{th,i}$ / ΔE_{mag} serves as a proxy for the ratio ion heating to cascading rate: Q_i / ϵ.

We assume that:
Injected energy (δB fluctuations) → Q_i + dissipation ($\sim Q_e$)

$$\frac{Q_i}{\epsilon} \sim \frac{Q_i}{Q_e}$$

(Arzamasskiy et al. 2019; Cerri et al. 2021; Arzamasskiy et al. 2023; Squire et al. 2022)

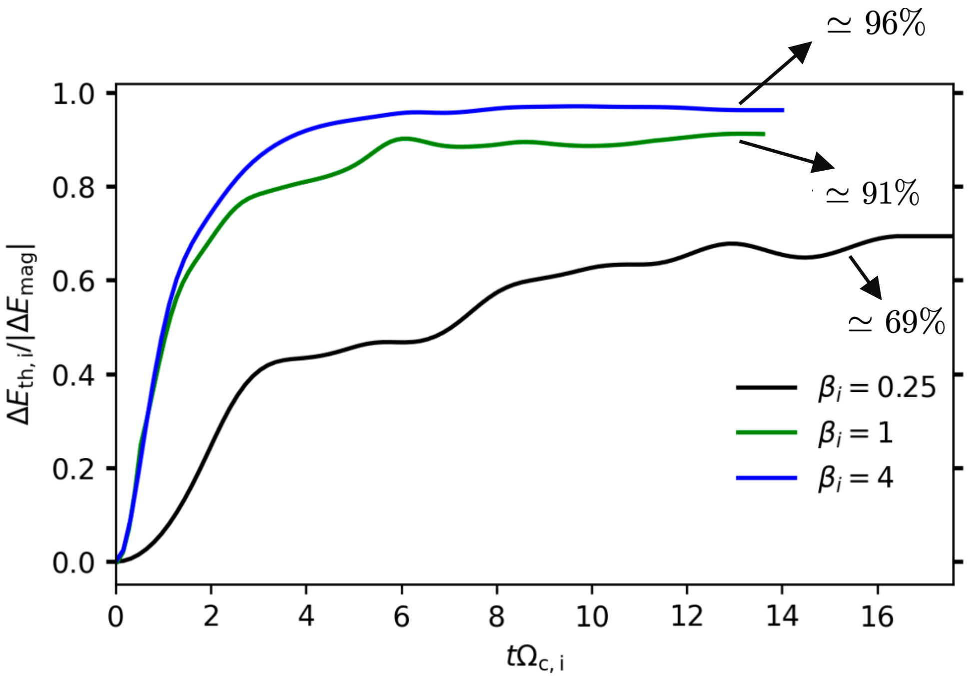

Comparison with Q_i/Q_e inferred from hybrid simulations of Pegasus++ with Alfvénic injection ($\delta B_{\|} = 0$), taken from Arzamasskiy et al. (2023):

- For $\beta_i = 0.25$: consistent with previous hybrid simulations.

- **For $\boldsymbol{\beta_i > 1}$: larger ion heating.**

Related to the difference in the injection scale, and compressibility of injected fluctuations.

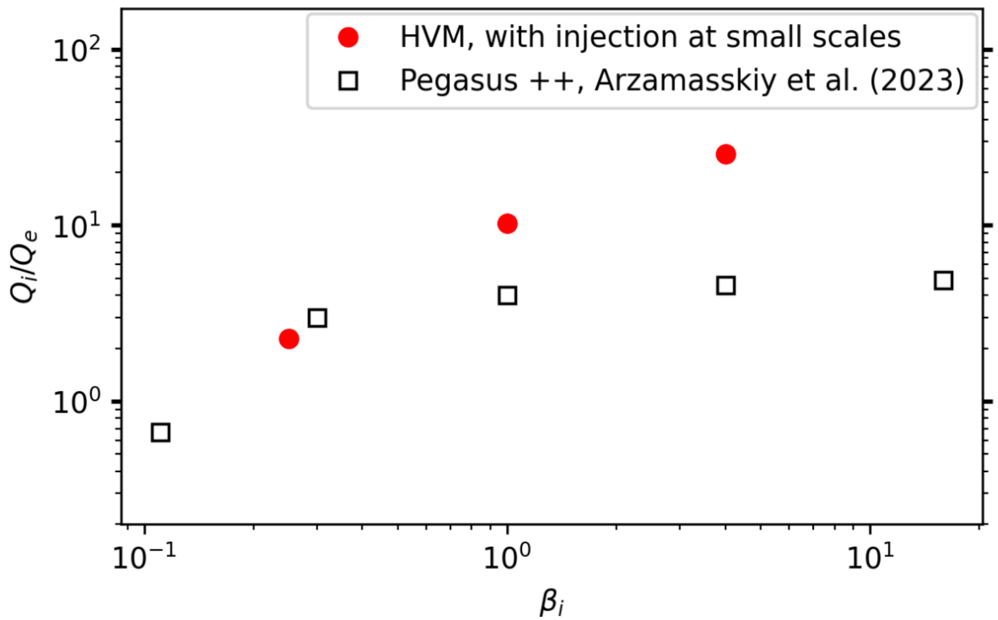

Conclusions:

- Transition from KAW to IKAW and then to IWW fluctuations at sub-ion scales.
- Velocity spectra show decoupling between ions and electrons as β_i increase.
- Anisotropic ion heating is observed. Ion-cyclotron instability (iCI) plays a role in controlling plasma temperature anisotropy.
- Larger fractions of cascading magnetic energy convert into ion heating as ion beta increases.
- Sensitivity of ion heating to scale separation between injection scales and ion gyroradius, and compressibility of injected fluctuations.

Thank you for your attention.